J Mater Sci (2006) 41:6460–6464
DOI 10.1007/s10853-006-0365-4

Magnetic and electrical properties of lanthanum substituted yttrium iron garnets

S. R. Nimbore · D. R. Shengule · S. J. Shukla · G. K. Bichile · K. M. Jadhav

Received: 25 March 2004 / Accepted: 7 July 2005 / Published online: 19 September 2006

Abstract Polycrystalline yttrium lanthanum iron garnets ($Y_3La_xFe_{5-x}O_{12}$) with varying La substitution ($0 \le x \le 0.5$) have been prepared in the pellet form, and studied by X-ray diffraction, magnetization, a.c. susceptibility and electrical resistivity measurements. The lattice constants are determined and the applicability of Vegard's law has been tested. The saturation magnetization ($4\ \pi M_S$) decreases very slowly almost linearly with increasing x from $x = 0.0$–0.5 indicating minimal reduction in ferrimagnetism and least magnetic loss. Variation of saturation magnetic moment per formula unit at 300 K with x can be explained satisfactorily assuming the collinear spin-ordering model. The Curie temperature (T_c) reduces very slowly with increasing x, which is consistent with the observed decrease in $4\ \pi M_S$ with x. The activation energy (E) decreases very slowly with increasing x for $x > 0.1$.

Introduction

Yttrium iron garret (YIG) is microwave ferrite, which in polycrystalline form has specific characteristics. Substituted yttrium iron garnets have found extensive use in wide band non-reciprocal devices [1]. In this family of microwave materials, polycrystalline Al substituted Yttrium garnets ($Y_3Al_xFe_{5-x}O_{12}$) have been used in devices where low loss is the major factor. There fore these systems ($Y_3Al_xFe_{5-x}O_{12}$) have been studied extensively by many investigators [2–5]. In our recent study of the Al–Cr co-substituted yttrium iron garnets ($Y_3Al_xCr_xFe_{5-x}O_{12}$) [6], we have observed that the saturation magnetization ($4\ \pi M_S$) indicates low losses satisfying the requirements of device engineers.

The aim of the present work is to develop sintered material of the rare earth like lanthanum substituted yttrium iron garnets ($Y_3La_xFe_{5-x}O_{12}$) and to study the effect of La substitution on the properties of YIG in meeting the requirements of device engineers. The present paper reports, the synthesis of $Y_3AI_xFe_{5-x}O_{12}$ ($x = 0.0$–0.5) and investigation of the structural, magnetic and electrical properties of these system through X-ray diffraction, magnetization, a.c. susceptibility and electrical resistivity measurements.

Experimental

Six samples of La substituted $Y_3La_xFe_{5-x}O_{12}$ garnets with $x = 0.0$–0.5 were prepared by the usual ceramic method. The starting materials were Y_2O_3, Fe_2O_3 and La_2O_3 all 99.9% pure supplied by E. Merck. The oxides were mixed thoroughly in stoichiometric proportions to yield the desired composition and wet ground. The mixture was dried and pressed into pellets. These pellets were presintered at 1,100 °C for 30 h in air and cooled to room temperature. The pellets were crushed into powders, reground, and palletized. Such pellets were calcined at 1,400 °C for 24 h and slowly cooled to room temperature to obtain garnet phase.

The powder X-ray diffraction (XRD) patterns for all the samples were recorded at room temperature with a PW 3710 diffractometer using Cr-K_α radiation and

S. R. Nimbore · D. R. Shengule · S. J. Shukla · G. K. Bichile · K. M. Jadhav (✉)
Department of Physics, Dr. Babasaheb Ambedkar Marathwada University, Aurangabad 431004 M.S., India

diffractograms showed sharp lines corresponding to a single phase garnet. The magnetization measurements were carried out by using high field hysteresis loop technique [7] at 300 K. The a.c. susceptibility measurements on powdered samples were made in the temperature range 300–700 K using double coil set-up [8] operating at a frequency of 110 Hz and in r.m.s. field of 0.5Oe. The electrical resistivity as a function of temperature was measured using a two-probe method for all samples in the form of pellets.

Results and discussion

Typical X-ray diffraction pattern (XRD) shown in Fig. 1 shows only the garnet lines suggesting single-phase behaviour. The analysis of the XRD pattern revealed that all the samples have a single-phase cubic structure. Lattice constants determined from XRD data with an accuracy of ±0.002 Å for x = 0.0–0.5 are shown in Fig. 2a as a function of x. The lattice constants exhibit a very slow linear increase with increasing x (Fig. 2a), thereby obeying Vegard's law [9]. The linear increase in lattice constant 'a' with La substitution is explained on the basis of difference in ionic radii of Fe^{3+} and La^{3+} ions. In the present case, smaller Fe^{3+} ions (0.67 Å) are replaced by larger La^{3+} ions (1.06 Å). The density of $Y_3La_xFe_{5-x}O_{12}$ have been calculated from the molecular weight and volume of the unit cell and the values are given in Table 1. The density increases slowly with increase of La concentration. The lattice constant of YTG (pure garnet) agrees well with the literature values [3, 6].

The saturation moment (σ_s) and the magnetization number n_B (the saturation magnetization per unit formula unit in Bohr magneton) at 300 K obtained from magnetization data for x = 0.0–0.5 are summarized in Table 1. From field dependence of magnetization and observed magnetic moments (Table 1), it is clear that the spontaneous magnetization decreases very slowly with x for x = 0.0–0.5. The saturation magnetization (4 πM_S) shown in Table 1 for La substituted YIG decreases very slowly with x. Figure 2b displays the relative variation of $M_S(x)/M_S(o)$ with Al [2], AI–Cr [6] and La concentration of substituted YIG. It is evident from Fig. 2 that the $M_S(x)/M_S(o)$ decreases with x at the rate of 15.5%, 5.0% and 3.0%, respectively, for $Y_3Al_xFe_{5-x}O_{12}$, $Y_3Al_xCr_xFe_{5-2x}O_{12}$ and $Y_3La_xFe_{5-x}O_{12}$.

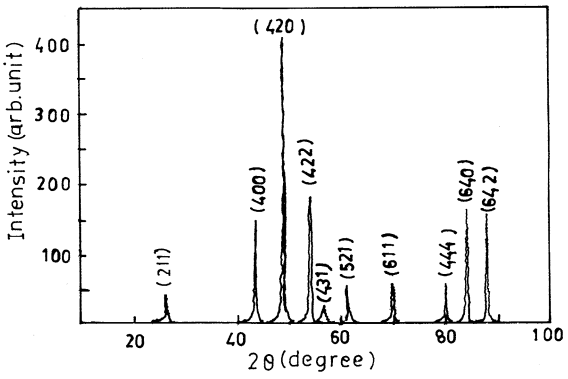

Fig. 1 Typical X-ray diffraction pattern for $Y_3La_xFe_{5-x}O_{12}$ with x = 0.2

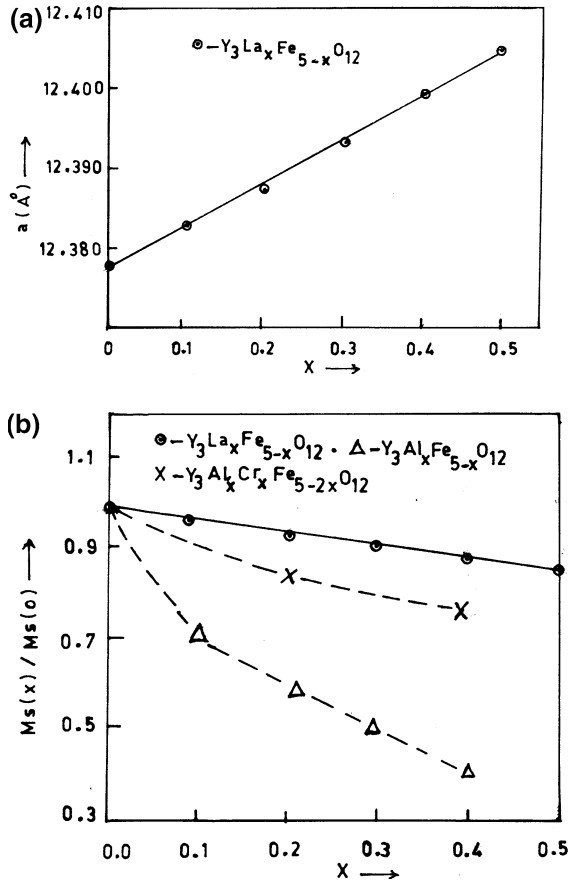

Fig. 2 (**a**) Variation of lattice constant a (Å), as a function of La content x in $Y_3La_xFe_{5-x}O_{12}$ (x = 0.0–0.5) (**b**) Variation of relative saturation magnetization $M_x(x)/M_S(o)$ with x in $Y_3Al_xFe_{5-x}O_{12}$, $Y_3Al_xCr_x$ $Fe_{5-x}O_{12}$ (6) and $Y_3La_xFe_{5-x}O_{12}$ systems

It is evident from Table 1 that, 4 πM_s decreases with increase in La substitution. Further the effect of La substitution in YIG shows least loss in 4 πM_S compared to Al [2] and Al-Cr [6] substituted YIG. Materials having high magneto–optical (M–O) properties exhibit least loss in 4 πM_S and such material are required for M–O devices like M–O memory and optical isolator.

Cations in the garnet crystal structure are arranged on three crystallographic sub-lattices [10] namely C-sites (dodecahedral), A-sites (octahedral) and D-sites (tetrahedral). The cation distribution for (YIG)-$Y_3Fe_5O_{12}$ [10] is usually expressed as,

Table 1 Lattice constant (a), X-ray density (d_x), saturation magnetization, Bhor magneton (n_B), Curie temperature T_c(K) from a.c. susceptibility and Activation energy E (eV) from resistivity for $Y_3La_xFe_{5-x}O_{12}$ garnet system

x	X-ray diffraction		Magnetization			Curie Temp. from a.c.susceptibility T_c (K)	Activation Energy From resistivity E (eV)
	a(Å)	d_x gm/cm^3	σ_s emu/gm	4 πM_s (G)	n_B (μ_B)		
0.0	12.377	5.165	39.55	2,568	5.23	550	0.32
0.1	12.382	5.222	37.08	2,434	4.95	534	0.35
0.2	12.386	5.276	35.84	2,377	4.84	528	0.33
0.3	12.393	5.324	34.61	2,312	4.73	517	0.32
0.4	12.398	5.396	33.37	2,263	4.61	480	0.24
0.5	12.404	5.410	32.14	2,181	4.49	460	0.20

$$\{Y_3\}^C[Fe_2]^A[Fe_3]^DO_{12} \quad (1)$$

The overall magnetization of YIG due to the three sub-lattices is given by,

$$M = (M_D - M_A) - M_C \quad (2)$$

Since Yttrium is non-magnetic, there is no moment due to C-sub-lattice i.e., $M_C = 0$. In YIG only A and D-sub-lattices contain magnetic ions Fe^{3+}. The moment due to one Fe^{3+} ion at 0 K is $5_{\mu B}$ and therefore the magnetization of YIG is $M = M_D$–$M_A = (3 \times 5 - 2 \times 5) = 5_{\mu B}$. At any temperature other than 0 K, the average moment M_A of the ions will be less than $5_{\mu B}$ due to thermal disorder, but the relation,

$$M = n_D m_D - n_A m_A = 3m_D - 2m_A \quad (3)$$

is still valid.

Comparing the site preference energies of the constituent ions [11] and X-ray data analysis, an approximate cation distribution $Y_3La_xFe_{5-x}O_{12}$ can be written as,

$$\{Y_3\}^C(Fe_{2-0.4x}La_{0.4x})^A[Fe_{3-0.6x}La_{0.6x}]^DO_{12}, \quad (4)$$

with x = 0.0–0.5.

According to Neel's two sub-lattice model of ferrimagnetism [12], the magnetic moment per formula unit in $_{\mu B}$, n_B^N at 0 K is expressed as

$$n_B^N(x) = M_D(x) - M_A(A) \quad (5)$$

where M_D and M_A are the D and A sub-lattice magnetic moments in μ_B. As Neel's model is applicable at 0 K, we have calculated the $n_B^N(x)$ for x = 0.0–0.5 using Eq. (4) and the values of $n_B^N(x)$ as a function of x are shown in Fig. 3. We have also displayed in Fig. 3 the measured values of $n_B(x)$ at 300 K (Table 1). The calculated $n_B^N(x)$ values for x = 0.0–0.5 are in good agreement with the experimentally found $n_B(x)$ values at 300 K (Fig. 3) confirming the collinear spin ordering.

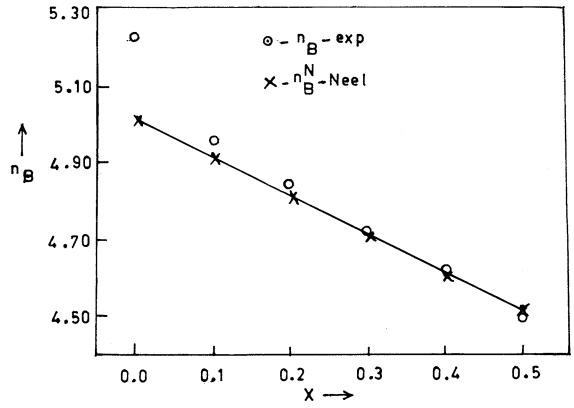

Fig. 3 Values of $n_B(x)$ as a function of x obtained from magnetization data at 300 K and the calculated $n_B^N(x)$ values with x from Neel's collinear model for $Y_3La_xFe_{5-x}O_{12}$

The temperature dependence of relative a.c. susceptibility $\chi_{ac}(T)/\chi_{ac}(RT)$ for typical sample with x = 0.1, 0.3 and 0.5 is shown in Fig. 4. The results of the a.c. susceptibility (Fig. 4) exhibit normal ferromagnetic ordering and the Curie temperature (T_c) obtained from it is listed in Table 1. The decrease in T_c with increasing x is consistent with the observed slow decrease in the saturation magnetization (4 πM_s) with x (Table 1).

The measured D.C. resistivity (ρ) for $Y_3La_xFe_{5-x}O_{12}$ system is carried out in the temperature range of 300–720 K. Plots of log ρ versus 1,000/T are shown in Fig. 5. log ρ versus 1,000/T plots (Fig. 5) for x = 0.0–0.5 exhibit a relatively sharp peak in electrical resistivity at a particular temperature T–T_{max} at which metal insulator transition is observed showing metallic type behaviour for $T < T_{max}$ and insulating behaviour for $T > T_{max}$. The activation energy (E) is calculated from the equation $\rho = \rho_0 \exp(-E/kT)$ in the semiconducting region ($T > T_{max}$) of x = 0.0–0.5 plots (Fig. 5) and are listed in Table 1. The values of activation energy are smaller as compared to Gd substituted YIG [13]. The lower values of activation energy may be due to intrinsic conduction in these materials. Figure 6 displays the variation of activation energy (E) versus x for

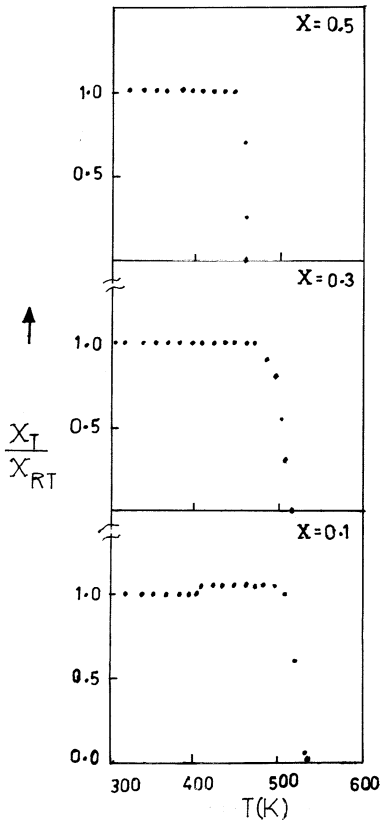

Fig. 4 Temperature dependencies of a.c. susceptibility ($\chi_{ac}(T)$/χ_{ac}(RT)) for $Y_3La_xFe_{5-x}O_{12}$ at x = 0.1, 0.3 and 0.5

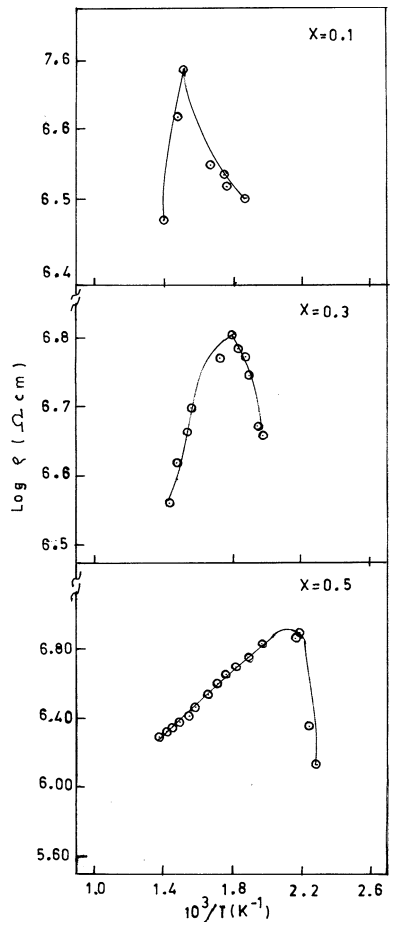

Fig. 5 Electrical resisitivity (log ρ) as a function of inverse temperature ($10^3/T$) for typical samples x = 0.0, 0.1, 0.4 and 0.5

$Y_3La_xFe_{5-x}O_{12}$ and $Y_3Al_xFe_{5-x}O_{12}$ [2]. It is evident from Fig. 6 that the activation energy (E) increases with increasing x linearly for $Y_3Al_xFe_{5-x}O_{12}$ with x = 0.0–0.4 [2] whereas the E values for $Y_3La_xFe_{5-x}O_{12}$ decrease slowly with increasing x for $x > 0.1$. This attributed to substitutional effects of rare earth La^{3+} ions. A noteworthy observation is that 4 πM_S, T_c and E values for $Y_3La_xFe_{5-x}O_{12}$ slowly decrease with increasing x from x = 0.1–0.5 exhibiting, respectively increase in metallic conductivity and least loss in ferrimagnetism similar to that of Ca, Sr, Ba substituted $LaMnO_3$ [14, 15].

Conclusions

The effect of La substitution in YIG shows that the saturation magnetization (4 πM_S) varies slowly from 2,568 to 2,181 Gauss for $Y_3Fe_5O_{12}$ (x = 0.0) to $Y_3La_{0.5}Fe_{4.5}O_{12}$ (x = 0.5) indicating least loss in 4 πM_S. The magnetic data can be explained assuming collinear spin ordering model. The Curie temperature (T_c) obtained from a.c. susceptibility decreases very slowly with increasing x. The activation energy (E) deduced from resistivity data shows very slow decrease with increasing x for $x \geq 0.1$ exhibiting enhancement of metallic type conductivity. The properties

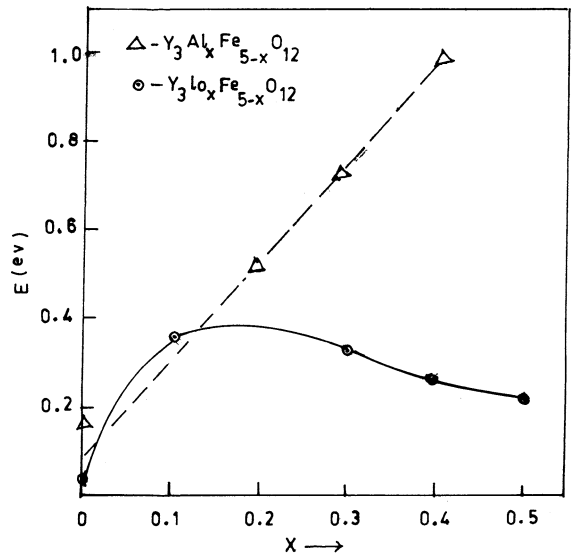

Fig. 6 Variation of activation energy (E) versus x for $Y_3Al_xFe_{5-x}O_{12}$ and $Y_3La_xFe_{5-x}O_{12}$

of $Y_3La_xFe_{5-x}O_{12}$ are better suited as compared to $Y_3Al_xFe_{5-x}O_{12}$ and $Y_3Al_xCr_xFe_{5-2x}O_{12}$ materials for microwave applications. Further La doped YIG has potential applications for magneto-optical devices.

Acknowledgements The authors are thankful to Professor R. G. Kulkarni, Dept. of physics, Shivaji University, Kolhapur, India for his valuable suggestion and fruitful discussion. The author is also thankful to USIC, Shivaji University, Kolhapur for providing X-ray diffractometric charts.

References

1. Lax B, Button K (1962) Microwave ferrities and ferri-magnetics, Mcgraw-hill book Co, Inc., New York
2. Srinivasan TT, Prakash O, Patni MJ (1981) Trans Ind Ceramic Soc 40(1):1
3. Suresh K, Patil KC (1994) J Alloys compounds 209:203
4. Microwave ferrities materials catalogue (1970) Trans. Tech. Incorporation, Graithsburge, Maryland, USA
5. Multani M, Nandikar NG, Venktraman N, Raghupathy V, Pansare AK, Gurjar A (1989) Meter Res Bull 14:1251
6. Murumkar VD, Modi KB, Jadhav KM, Bichile GK, Kulkarni RG (1997) Mat Lett 32:281
7. RadhaKrishanamurthy C, Likhite SD, Sastry P (1971) Phil Mag 23:503
8. RadhaKrishanamurthy C, Likhite SD, Sahstrabudhe P (1978) Proc Indian Acad Sci 87A:245
9. Whinfrey CG, Eckrot DW, Touber A (1982) J Am Chem Soc 82:2695
10. Hudson AS (1970) J Phys D Appl phys 3:251
11. Miller A (1959) J Appl Phys 30:145
12. Neel L (1950) CR Acad Sci Paris 230:375
13. Bahadur D, Prakash OM, Kumar D (1981) Bull Mater Sci 3:325
14. Van Hemlot R, Wercker J, Holzafel B, Shultz L, Samwer K (1993) Rev Lett 71:2331
15. McGramack M, Jin S, Tiefel TH, Fleming RM, Philips JM, Ramesh R (1994) Appl Phy Lett 64:3045